

Imaging and Locating Buried Tunnels Using a High-Resolution S-wave Seismic Survey Feasibility Field Test From Netherlands

Draganov, D.; Ghose, R.; Harmankaya, U.; Kaslilar, A.; Van der Burg, D.; Schoolderman, A.

DOI

[10.3997/2214-4609.202320026](https://doi.org/10.3997/2214-4609.202320026)

Publication date

2023

Document Version

Final published version

Published in

3rd Conference on Geophysics for Infrastructure Planning, Monitoring and BIM

Citation (APA)

Draganov, D., Ghose, R., Harmankaya, U., Kaslilar, A., Van der Burg, D., & Schoolderman, A. (2023). Imaging and Locating Buried Tunnels Using a High-Resolution S-wave Seismic Survey: Feasibility Field Test From Netherlands. In *3rd Conference on Geophysics for Infrastructure Planning, Monitoring and BIM: Held at Near Surface Geoscience Conference and Exhibition 2023, NSG 2023 EAGE*. <https://doi.org/10.3997/2214-4609.202320026>

Important note

To cite this publication, please use the final published version (if applicable). Please check the document version above.

Copyright

Other than for strictly personal use, it is not permitted to download, forward or distribute the text or part of it, without the consent of the author(s) and/or copyright holder(s), unless the work is under an open content license such as Creative Commons.

Takedown policy

Please contact us and provide details if you believe this document breaches copyrights. We will remove access to the work immediately and investigate your claim.

Green Open Access added to TU Delft Institutional Repository

'You share, we take care!' - Taverne project

<https://www.openaccess.nl/en/you-share-we-take-care>

Otherwise as indicated in the copyright section: the publisher is the copyright holder of this work and the author uses the Dutch legislation to make this work public.

Imaging and Locating Buried Tunnels Using a High-Resolution S-wave Seismic Survey: Feasibility Field Test From Netherlands

D. Draganov¹, R. Ghose¹, U. Harmankaya², A. Kaslilar³, D. Van der Burg⁴, A. Schoolderman⁴

¹ Department of Geoscience and Engineering, Delft University of Technology; ² Geophysical Engineering, Graduate School of Science Engineering and Technology, Istanbul Technical University; ³ Department of Earth Sciences, Uppsala University; ⁴ TNO, The Hague

Summary

Knowing the location and characteristics of shallow subsurface structures like tunnels, cavities, archeological ruins, etc. is of importance for different disciplines and application. To image and/or characterize such objects of interest, different geophysical methods are used. For imaging of a very shallow network of tunnels, the high-resolution seismic method with active sources provide valuable information. We show the results of analysis of an S-wave profile recorded over a network of very shallow tunnels in the Netherlands. The survey used a high-frequency vibratory S-wave source and horizontal particle-velocity geophones, both oriented in the crossline direction, along three lines. We process the reflection data along one of the lines to obtain a stacked section in depth. We also use a method inspired by seismic interferometry to localize a scatterer along the line. We show that both techniques image well the subsurface structures taking into account the 3D ambiguity of processing 2D data.

Imaging and Locating Buried Tunnels Using a High-Resolution S-wave Seismic Survey: Feasibility Field Test From Netherlands

Introduction

The imaging and characterization of very shallow structures like tunnels, cavities, archeological ruins, etc. is important for archeology, police, engineering applications, but also for mitigating hazards. For imaging and characterization, the power of the near-surface geophysical methods can be harnessed using, e.g., ground penetrating radar (Al-Fares *et al.* 2002), microgravity and multi-channel analysis of surface waves (Debeglia *et al.* 2006), seismic refraction and/or electric resistivity (Cardarelli *et al.* 2010) methods. The seismic reflection method with active sources can also be quite useful in many cases. For very shallow targets and soft sand/clay geology, a high-resolution S-wave survey might provide the best images. Due to the shorter wavelength of S-waves compared to P-waves for the same frequency, S-waves provide relatively higher resolution. Another practical reason is, that a line survey with S-wave sources and receivers oriented in the crossline direction, i.e., when performing an SH-wave survey, the SH-waves theoretically decouple from the P/SV-waves and thus the survey data could be processed as “acoustic” data, with the benefit of less complications due to conversions.

Survey

In September 2019, we performed a high-resolution active-source SH-wave seismic survey in the Netherlands over a network of shallow tunnels (Figure 1a) with the aim to test how this survey could be used for imaging/locating tunnels. We used S-wave sources and horizontal particle-velocity receivers oriented in the crossline direction. As a source, we used an S-wave vibrator (Ghose *et al.* 1996; Brouwer *et al.* 1997). The acquisition geometry represented three receiver lines (labeled Line 1 to Line 3 in Figure 1b) of 10-Hz horizontal geophones spaced at 0.5 m. The source points were only along Line 1 and Line 2 with source spacing of 1 m. The first source position along Line 1 was 3 m before the first geophone position along this line (lowest blue dot in Figure 1b). The first source position along Line 2 was at the first geophone position along this line (right-most blue dot in Figure 1b). All three lines were recording the signals from each source.

There are three lines of buried tunnels known to be aligned parallel to Line 1 and visible by the vertical-shaft covers in Figure 1b – one to left of and with the closest wall ~ 3.6 m horizontally away from the line; one to the right of and with the closest wall ~ 3.3 m horizontally away from the line; one further to the right and with the closest wall ~ 10.6 m horizontally away from the line. Line 2 passes above these three buried tunnels.

There are four lines of tunnels perpendicular to Line 1 and passing under it along the vertical axis in Figure 1b between ~ 3.5 m and ~ 5.9 m, ~ 17 m and ~ 18.4 m, ~ 28.2 m and ~ 30.2 m, and ~ 34.3 m and 35.8 m.

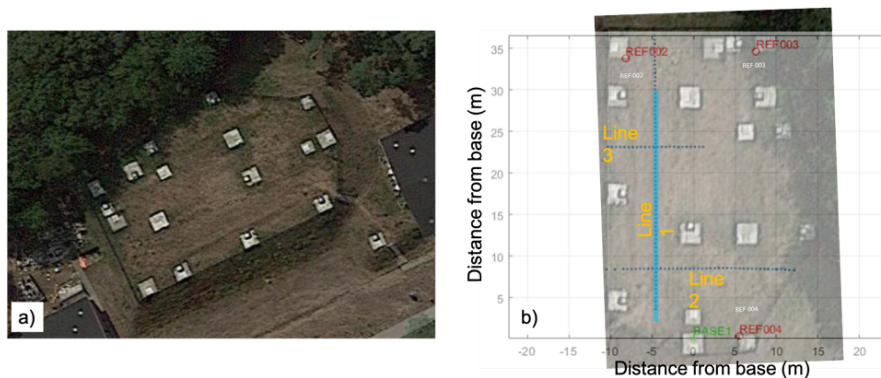


Figure 1 (a) Top view of the surface situation above the system of tunnels. (b) The three receiver lines (dark blue dots; marked Line 1,2,3) overlaid on the rotated top view from a). REF002, REF003, and REF004 – the three reference points used to tie the coordinates of the seismic lines; BASE1 – point zero for the coordinate system; light blue line – spatial extent of the stacked section of Line 1.

Results

The vibroseis raw data were compressed using a source monitor trace derived from data of several sensors that were placed on the body of the source. The data were then processed using two approaches: 2D reflection imaging for obtaining an image of the tunnels below Line 1 and Line 2; locating scatterers using 2D data.

Figure 2a shows representative common-shot gathers for three different shot locations (shot positions 5, 18, and 29) along Line 1. We can clearly see the linear direct waves and high-amplitude Love waves, but also the presence of hyperbolic, shallow reflection events is apparent in the raw field shot gathers. We preprocess the raw common-shot gathers to increase the signal-to-noise ratio of the shallow reflection events through filtering and/or suppressing undesirable events. For this dataset, the surface waves have slightly lower frequency than the predominant frequency of the shallow reflections. In common-shot gathers, in the far offsets the velocity of the surface waves approaches that of the hyperbolic reflection events. It is, therefore, difficult to remove the surface waves by simple bandpass filtering or frequency-wavenumber (f-k) filtering without disturbing the S-wave reflections. Thus, to suppress the surface waves in this situation, we mute the direct waves, apply spectral balancing to accentuate the reflections and suppress the surface-wave energy, and finally – in the step of velocity analysis – we use a root-mean-square velocity which preferentially stacks the reflections and suppresses further the surface waves. To prevent artefacts, we restrict the preprocessing to the minimum essential steps: (i) killing dead traces and reversing wrong-polarity traces; (ii) top muting to remove much of the direct and anti-causal events; (iii) spherical divergences and intrinsic attenuation correction; (iv) spectral shaping; (v) automatic gain correction. Figure 2b shows the common-shot gathers from Figure 2a but after the preprocessing. Some surface wave energy still remains; however, the hyperbolic reflection events and some diffraction events, possibly from localized scatterers, have become quite clear. Two reflection events at zero-offset time of about 40 ms and 75 ms are visible. The two red-dashed circles in Figure 2b mark two diffraction events.

We then re-sort the reprocessed common-shot gathers into common-midpoint gathers, and use a series of constant-velocity stacks to identify which velocity stacks preferentially suppress the surface waves and at the same time accentuates the shallow reflections at different two-way traveltimes. Accordingly, we choose a 1D velocity function that suppresses the surface waves and stacks best the reflections events. For this dataset, a stacking velocity of 165 m/sec at 0 s with a small positive velocity gradient with time is found to give the best result.

Figure 2c shows the stacked section after normal-moveout correction. The beginning of the section is at ~2 m along the vertical axis in Figure 1b. The events visible in this stacked section represent primarily body-wave reflections and scatterers. The 45 and 75 ms two-way-traveltime reflection events are nicely stacked. In Figure 2d, we also indicate in red three prominent scatterers. The scatterers in the shot gathers in Figure 2b are at the same lateral location and at the same time (for the apex) as the scatterers imaged in the stacked section, thus lending credence to our interpretation. Judging from the tentative depth in Figure 2c, the two left scatterers could be indicating edges of the tunnel structures at those locations from the two closest tunnels running parallel to Line 1. The prominent horizontal reflectors correspond well in tentative depth with expected side reflections from the three tunnels parallel to Line 1. Taking into account the depths to the different parts of the tunnels at approximately 1.3 m, 3.6 m, and 6.3 m, the expected tentative depths in the 2D section in Figure 2d are of approximately 3.6 m, 3.9 m, 4.9 m, 7.3 m, 10.7 m, and 11.2 m. The stacked section passes above the first three perpendicular tunnels. The reflections from them would be imaged as diffractors or short reflectors, like the events till 3 m and around 15 m along the stacked section in Figure 2d. These events interfere in the stacked section with the events from the parallel tunnels.

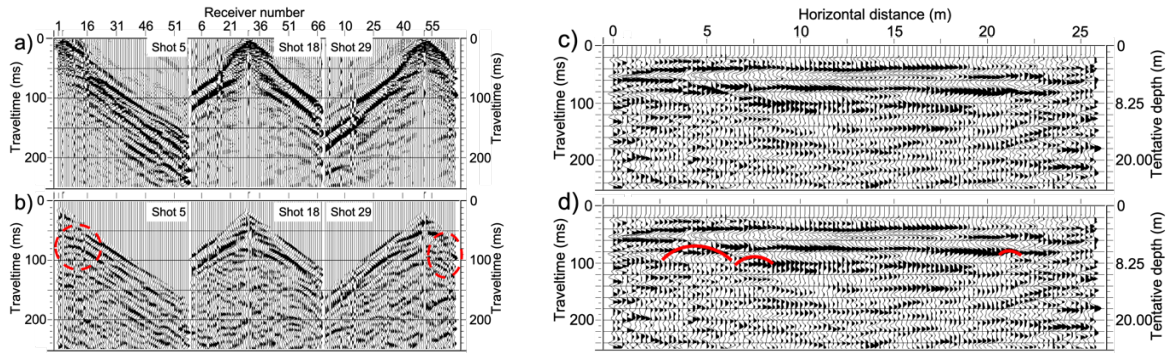


Figure 2 (a) Example common-shot gathers for three shot positions along Line 1. (b) The same common-shot gathers after preprocessing. The red-dashed circles indicate diffraction events. (c) Stacked section from Line 1. (d) The same stacked section with indication of three scatterers in red. The spatial extent of the stacked section is indicated in Figure 1b in light blue.

To locate scatterers, we used a method based on cross-correlation of isolated scattered body or surface waves (Harmankaya *et al.*, 2013; Kaslilar *et al.* 2013, 2014; Harmankaya *et al.* 2018) inspired by seismic interferometry. Suppose a surface line of geophones has recorded the response due to a surface source from a subsurface containing one scatterer. The recording then represents a common-source gather with direct/surface waves, the scattering arrival, and possibly also reflections and refractions. The method uses the scattering arrival by extracting one of the traces containing this arrival and correlating this trace with the complete common-source gather. The cross-correlation process subtracts the traveltime from the source through the scatterer to the geophone at whose position the trace was extracted. This leaves traveltime differences (both positive and negative differences are possible) at the traces with respect to the extracted trace. Effectively, the cross-correlation has completely eliminated the travel path between the source and the scatterer. In this way, the estimation of the scatterers' location using the obtained traveltime differences becomes independent of the source location and depends only on the properties between the scatterer and the receivers. By inversion of the obtained traveltime differences, using a velocity value between the scatterer and the receivers, the location of the scatterer is estimated.

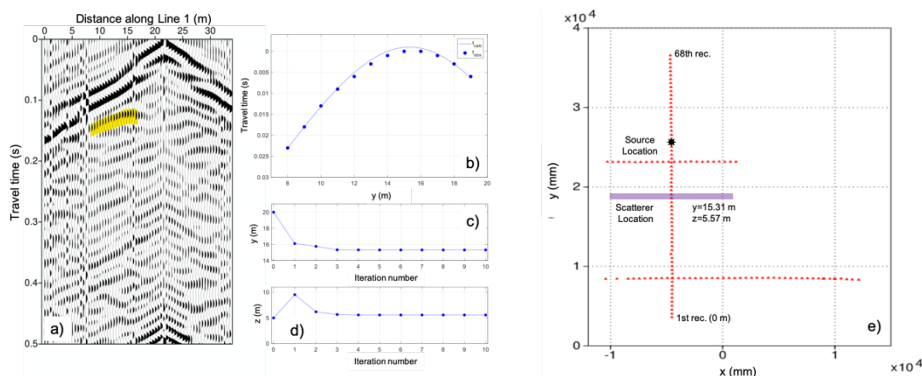


Figure 3 (a) Band-pass filtered between 1 Hz and 40 Hz and after-AGC common-shot gather along Line 1 from shot at 22 m: yellow stripe indicates chosen scattering arrival. (b) Inversion result using a velocity of 150 m/s: blue dots – picked times; blue line – calculated times. (c) Estimated distance of the scatterer along Line 1 from the beginning of the line as a function of the iteration number. (d) Estimated depth of the scatterer below Line 1 from the surface as a function of the iteration number. (e) Plan view of the estimated scatterer location with respect to the three acquisition lines (red triangles): black star – source location; purple stripe – diameter of the semi-circle representing the 3D depth ambiguity.

Figure 3a shows a shot gather that we use to locate a scatterer with the chosen scattering event indicated in yellow. Using this event with the above-explained method, we estimate the horizontal and depth

location given in Figures 3c,d, respectively, as a function of iteration number; Figure 3b shows the picked traveltimes and the traveltimes calculated by the inversion. The estimated distance along Line 1, starting from the beginning of the line, is ~15.3 m, which corresponds to ~17.4 m from the base. This fits very well with the location of one of the tunnels crossing perpendicularly Line 1. The estimated depth of ~5.6 m is close to the depth of ~6.3 m of this tunnel. The inversion assumes a pure 2D recording, which means that we deal with the 3D ambiguity of the depth inversion. That is why, in Figure 3e we show by the purple line the diameter of the semi-circle indicating this ambiguity. The purple line passes through one of the vertical-shaft covers indicating that the scattering event might be resulting from this shaft as well.

Conclusions

We performed a high-resolution seismic reflection survey along three lines for imaging and characterization of a network on very shallow tunnels. To perform an SH-wave survey, we used a vibratory S-wave source and horizontal particle-velocity geophones oriented in the cross-line direction. We applied 2D reflection processing to obtain a stacked section below the longest line. The two-way traveltime was converted to tentative depth using a stacking velocity of 165 m/sec at 0 s with a small positive velocity gradient. The stacked section exhibited several imaged reflectors and diffractors. These correspond well with the approximate depth in 3D of the walls of three buried tunnels that run parallel to the line, but also with the depth to the top of the tunnels crossed by the line. We also located scatterers using the data along this same line and a method inspired by seismic interferometry. We extracted one scattering event, and estimated its location and depth. Due to the 3D ambiguity of the location technique, the location indicates either one of the tunnels crossing perpendicular to the line or a vertical shaft from this tunnel coming to the surface at one side of the line.

References

- Al-Fares, W., Bakalowicz, M., Guérin, R., and Dukhan, M. [2002] Analysis of the karst aquifer structure of the Lamalou area (Hérault, France) with ground penetrating radar. *Journal of Applied Geophysics*, **51**, 97–106.
- Brouwer, J., Ghose, R., Helbig, K. and Nijhof, V. [1997] The improvement of geotechnical subsurface models through the application of s-wave reflection seismic exploration. *EEGS 3rd Annual Meeting*, Extended Abstracts, 103-106.
- Cardarelli, E., Cercato, M., Cerreto, A., Di Filippo, G. [2010] Electrical resistivity and seismic refraction tomography to detect buried cavities. *Geophysical Prospecting*, **58**(4), 685–695.
- Debeglia, N., Bitri, A., Thierry, P. [2006] Karst investigations using microgravity and MASW: application to Orleans, France. *Near Surface Geophysics*, **4**, 215–225.
- Ghose, R., Nijhof, V., Brouwer, J., Matsubara, Y., Kaida, Y. and Takahashi, T. [1998]. Shallow to very shallow, high-resolution reflection seismic using a portable vibrator system. *Geophysics*, **63**, 1295-1309.
- Harmankaya, U., Kaslilar, A., Thorbecke, J., Wapenaar, K., and Draganov, D. [2013] Locating near-surface scatterers using non-physical scattered waves resulting from seismic interferometry. *Journal of Applied Geophysics*, **91**, 66–81.
- Harmankaya, U., Kaslilar, A., Wapenaar, K., and Draganov, D. [2018] Locating scatterers while drilling using seismic noise due to tunnel boring machine. *Journal of Applied Geophysics*, **152**, 86–99.
- Kaslilar, A., Harmankaya, U., Wapenaar, K., and Draganov, D. [2013]. Estimating the location of a tunnel using correlation and inversion of Rayleigh wave scattering. *Geophysical Research Letters*, **40**, 6084–6088.
- Kaslilar, A., Harmankaya, U., van Wijk, K., Wapenaar, K., and Draganov, D. [2014]. Estimating location of scatterers using seismic interferometry of scattered Rayleigh waves. *Near Surface Geophysics*, **12**, 721–730.